American Iron and Steel Institute–Federal Highway Administration Model Bridge Test

MARK MOORE AND IVAN M. VIEST

The Model Bridge Study involved a large experimental test program to evaluate the behavior of a 0.4-scale model of a two-span continuous plate-girder bridge with modular precast prestressed deck panels. The bridge was designed according to the alternate load factor design (ALFD), or autostress, procedures. The project was jointly sponsored by the Federal Highway Administration (FHWA) and the American Iron and Steel Institute (AISI). Initiated in late 1982, the model bridge project was part of a comprehensive research program conducted by AISI to extend inelastic design procedures to continuous girders with noncompact elements. The American Association of State Highway and Transportation Officials (AASHTO) guide specification for ALFD procedures permitted the use of inelastic design methods only for bridges made of braced compact sections. In the model bridge test program, elastic lateral live-load distribution was studied at the service load level. At the overload and maximum load levels, the adequacy of the ALFD limit-state criteria to satisfy related structural performance requirements was analyzed. The behavior of the concrete slab made of precast deck panels was studied at all three load levels.

The model bridge study involved a large experimental test program to evaluate the behavior of a 0.4-scale model of a two-span continuous plate-girder bridge with modular precast prestressed deck panels. The bridge was designed according to the alternate load factor design (ALFD), or autostress, procedures. The project was jointly sponsored by the Federal Highway Administration (FHWA) and the American Iron and Steel Institute (AISI). Initiated in late 1982, the model bridge project was part of a comprehensive research program conducted by AISI to extend inelastic design procedures to continuous girders with noncompact elements. The American Association of State Highway and Transportation Officials (AASHTO) guide specification of ALFD procedures permitted the use of inelastic design methods only for bridges made of braced compact sections (*1*).

The principal goals of the research program were to study the behavior of

1. A two-span continuous plate-girder bridge designed according to ALFD procedures but built with noncompact elements, and
2. A concrete bridge slab made of modular precast panels prestressed in both directions and connected to the continuous steel superstructure to provide composite action.

M. Moore, Wiss, Janney, Elstner Associates, Inc., 2189 Northlake Parkway, Suite 100, Atlanta, Ga. 30084. I. M. Viest, IMV Consulting, P.O. Box 1428, Bethlehem, Pa. 18016.

The model bridge, shown in Figure 1, was subjected to a series of tests at each of the three AASHTO design load levels: service load, overload, and maximum load (*2*). In addition, a series of simulated single and tandem axle loads were applied to evaluate the performance of the precast deck. Further information on those aspects of the project that are not covered in this paper can be found in reports by Moore et al. (*3–8*). This paper is a review of the performance of the model bridge. Observed behavior of the model at each of the three AASHTO load levels is presented and compared with anticipated performance.

TESTS OF MODEL BRIDGE

Service Load

At the service load level, the response of the bridge was evaluated under wheel loads, truck loads, and lane loadings. Wheel load distribution, development of automoments, rotation capacity, and relative contribution of deck and crossframes to the live-load distribution were investigated.

One of the main objectives of the service load testing was to determine the influence surfaces and distribution coefficients for reactions and moments of a multigirder bridge. The test results were compared with theoretical predictions obtained from a finite element analysis and with the requirements of the AASHTO specifications (*2*).

Overload

At the overload level, the model bridge was subjected to a series of simulated truck and lane loadings. The main objective was to determine the shake-down behavior of the model bridge under repeated applications of the overload and the inelastic moment-rotation relationship for the girders.

In load factor design (LFD), permanent deformations are controlled by limiting the maximum elastic overload stress to $0.80F_y$ in noncomposite sections and $0.95F_y$ in composite sections (*2*). These stress limits were developed decades ago based on tests conducted by the American Association of State Highway Officials (AASHO) Road Test (*9*). Although these stress limits were based on tests of simple-span bridges, the AASHTO specifications do not limit their application to positive-moment sections. When applied in the negative-moment regions at interior supports of continuous spans, stresses at overload are generally limited to $0.80F_y$ because of the frequent use of noncomposite sections over the sup-

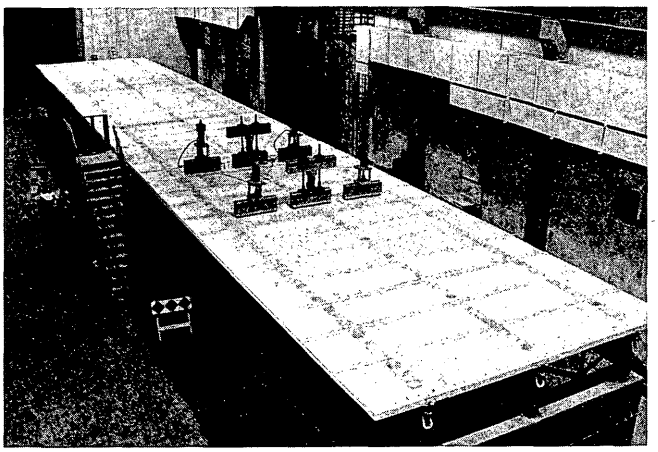

FIGURE 1 Overall view of model bridge.

ports. This limitation encourages the use of cover plates in negative-moment regions of rolled beams and of heavier flange plates in welded beams to satisfy the elastic moment envelope. Such practice increases cost of fabrication and can have a deleterious effect on fatigue strength of the bridge.

ALFD recognizes that there is no need to limit the elastic stresses at overload in negative-bending at interior supports of continuous beams. Minor local yielding at interior supports causes the excess pier moments to redistribute to positive-moment sections. To control permanent deformations, the stress limits of $0.80F_y$ for noncomposite sections and $0.95F_y$ for composite sections are applied after redistribution, but only at positive-moment sections. The plastic rotations that result at interior piers because of the local yielding shake down with a few passages of the overload vehicle so that the bridge response becomes elastic again.

The small plastic rotations at interior piers result in the formation of a set of beneficial self-equilibrating support reactions and corresponding moments that, along with the dead-load reactions and moments, remain in the structure after the live-load is removed. These redistribution moments, termed "automoments," reduce the peak support moments and increase the moments in the spans. The redistribution ensures that the structure shakes down and responds elastically after a few passages of the overload vehicle. The formation of these redistribution moments and the shake-down phenomenon have been previously observed experimentally (*10*).

Maximum Load

At the maximum load level, the model bridge was subjected to simulated lane loads over two girders. The primary purpose of this testing was to determine if the mechanism analysis based on the effective plastic moment M_{pe} was adequate for the strength prediction of a continuous bridge (*11*). In addition, the maximum load tests were designed to evaluate both the inelastic moment-rotation behavior of a continuous bridge in the positive- and negative-bending regions, and the lateral live-load distribution at the rated AASHTO maximum load.

Subsequently, the simulated lane loads were increased until the bridge could resist no additional load. This further testing was designed to establish the ultimate strength of the model bridge and to evaluate how well the ALFD procedures, based on the effective plastic moment concept, estimate the ultimate capacity of the bridge.

DESIGN AND DESCRIPTION OF MODEL

The initial step in the project was to design a prototype bridge and to scale it down to the model bridge. The dimensions of the model were determined by the physical characteristics of the FHWA Structures Laboratory at McLean, Virginia; fabrication techniques; and availability of plate material. On the basis of these limitations, a 0.4-scale factor was selected. An elevation view of one span is shown in Figure 2 and a cross section is shown in Figure 3. The model bridge had two 56-ft (17-m) spans, a transverse girder spacing of 6 ft 9⅝ in. (2 m), and 2 ft 9$^{9}/_{16}$ in. (0.85-m) deck-panel overhangs. Except for the bottom flanges in the outer 11 ft 2 in. (3.4 m), the plate girder dimensions were constant throughout the full length of the bridge: top flange ¼ in. by 5⅝ in. (6 mm by 140 mm), web ¼ in. by 27$^{3}/_{16}$ in. (6 mm by 690 mm), and bottom flange $^{9}/_{16}$ in. by 8 in. (14 mm by 200 mm). The precast panels of the slab were connected to the steel girders with stud shear connectors welded through preformed holes. The spaces around the connectors and between the underside of the panels and the top surface of the steel girders were filled with grout. For additional details see Moore et al. (*5–8*).

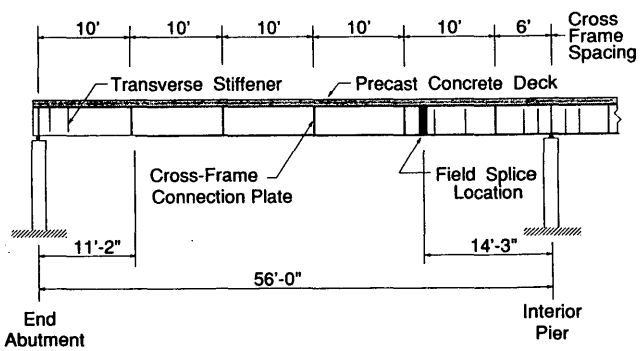

FIGURE 2 Elevation of model bridge.

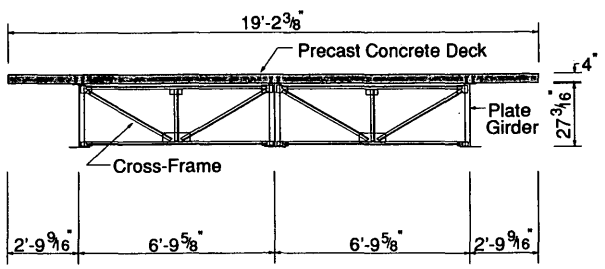

FIGURE 3 Cross section of model bridge.

PERFORMANCE OF MODEL BRIDGE

Service Load Tests

The service load behavior of the model bridge is illustrated by the contour lines of elastic influence surfaces shown in Figures 4 and 5. The elastic moments caused by a single concentrated load in each girder at the interior-pier and maximum positive moment sections were computed from measured strain data. These girder moments were then compared with the moments computed using a three-dimensional finite element model. The influence surface for the moment at a girder section was defined by the values of that moment for a unit load applied at 77 points. Each moment value was plotted at the corresponding load point.

The agreement between the measured and analytical ordinates was generally good. The measured ordinates were consistently smaller. This may be because (a) in the test the load was applied over a finite area, whereas in the finite element model the load was applied at a nodal point; and (b) the finite element model may have resulted in an overly stiff representation of the girders because of the assumptions that the girder cross section did not distort, the deck was rigidly connected to the girder, the web had no initial distortions, and the web did not compress vertically at the load and reaction points.

Overload Tests

Simulated truck loads equivalent to 100 percent of the AASHTO overload were applied first. Four different simulated truck loads were needed to obtain maximum positive moments for both the outside and inside girders in each span. They were followed by two different simulated lane-loads to induce maximum negative moments. After this first cycle of live loading, second and third cycles were applied in the same sequence as the first.

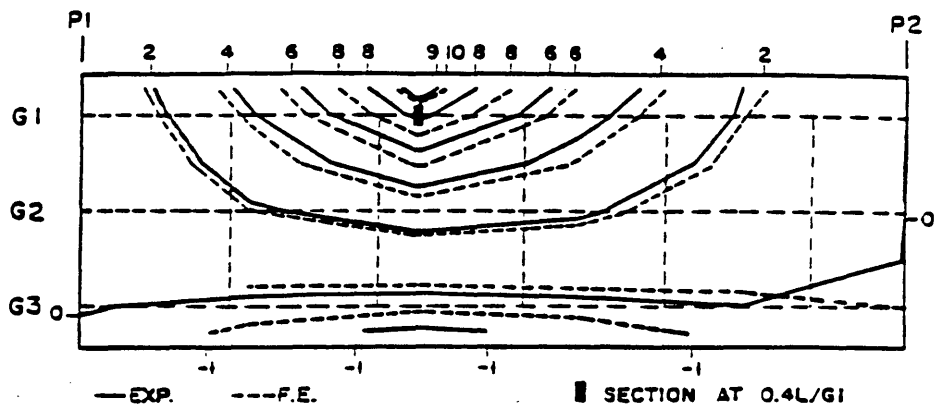

FIGURE 4 Comparison of measured and calculated influence surfaces for moment for girder *G*1 at 0.4*l*; load applied on west span.

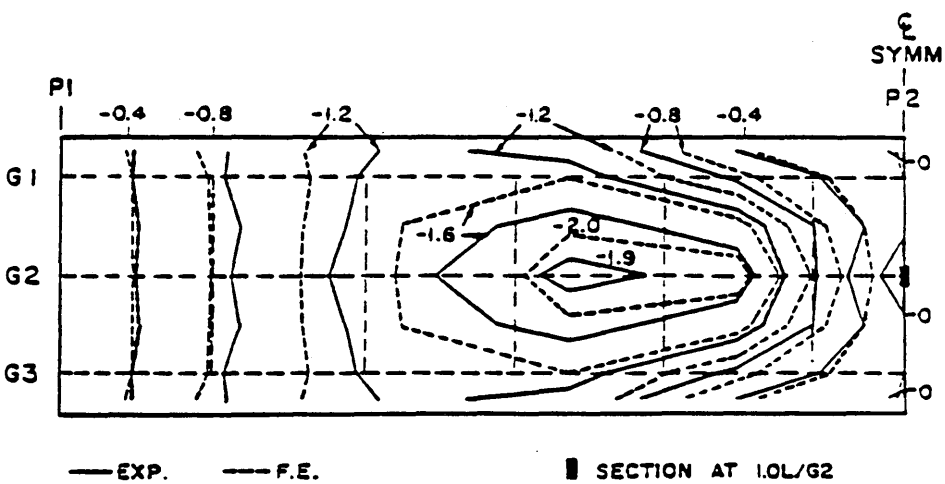

FIGURE 5 Comparison of measured and calculated influence surfaces for moment of girder *G*2 at 1.0*l*; load applied on west span.

During the first cycle, the simulated truck and lane live loads were applied in several increments and the resulting changes of strains in regions of maximum positive and negative bending were recorded. In subsequent cycles, the loads were increased directly from 0 to 100 percent.

The difference in the measured reactions before and after overload testing at each line of bearings can be considered to be the autoforces, or reactions, caused by the automoments. The average of the total automoment reactions at the abutments was approximately equal to one half the total automoment reaction at the center pier. The average total automoment reaction at the abutments times the span length gave a total positive automoment across the interior-pier bearing line of 201.7 kip-ft (270 kN-m). The total pier automoment represented about 8.7 percent of the sum of the total elastic overload pier moments. Only slight increases in the deformations of the girder webs and bottom (compression) flanges were observed at overload.

Cracking of the precast panels was observed only in the panel directly over the interior pier. The observed cracks were less than 7 mils (0.2 mm) wide, and closed when the live load was removed. The cracks were generally observed to initiate from the corners of the grouted blockouts. There were no cracks observed in the panel-to-panel joints. After all girders had shaken down with the maximum stress in positive bending in the most heavily loaded girder at approximately $0.95F_y$, the girder camber, which included the anticipated camber caused by the automoments, was essentially 0. Thus, the ALFD limit-state criteria were found to satisfy the overload structural performance requirement.

Service Load Tests After Overload

An important element of the ALFD procedure relates to the limited yielding permitted at the AASHTO overload level, and the subsequent elastic behavior of the bridge. The stresses in the steel girders at overload are limited to $0.95F_y$ in positive bending, with yielding permitted in the negative moment regions. However, the performance criteria in ALFD require good rideability of the bridge following repeated applications of the overload. Thus the permanent deformations associated with the shakedown must remain very small.

To verify the desired elastic behavior of the bridge following the overload and shake-down tests, concentrated loads were applied at a series of selected locations on the bridge. For each load location, the measured reactions were compared with those obtained for the same loading and locations in tests conducted before the overload testing. The differences between the two sets of identical tests were small, as is illustrated in Figures 6 and 7. They varied from 0 to about 15 percent.

Although not directly related to the extension of ALFD to noncompact plate girders, the model bridge study included a series of tests to evaluate the effect of cross-frames on the lateral live load distribution characteristics of the bridge. Selected cross-frames were removed and the series of tests with a single concentrated load was repeated. Comparisons of measured reactions and forces in instrumented cross-frames in these two sets of identical tests are shown in Figures 8 and 9. In the exterior girder the moments remained essentially unchanged whereas in the interior girder the moments increased up to about 15 percent when the cross-frames were removed.

Maximum Load Tests

The single structural performance requirement at maximum load is that the bridge must be able to resist the load without collapse. To determine the adequacy of the plastic mechanism analysis using M_{pe} for the strength prediction of a continuous bridge at maximum load, the model bridge was subjected to a simulated rated AASHTO maximum load lane loading. For this particular bridge configuration, lane loading was determined to be more critical for mechanism formation because it causes larger rotations at the interior pier than truck loading. After adding dead load to simulate the theoretical 30 percent increase of dead load specified by AASHTO at maximum load, the simulated lane loads were increased in increments until the measured critical bottom-flange bending stress in the positive-moment region of the most heavily loaded girder equaled the static yield stress. This represented the LFD limit state for noncompact girders in positive bending at maximum load and, therefore, the rated load. The loads were then increased further in the given proportions to determine how much reserve strength was available in the bridge above the rated load. Simulated lane loads for critical loading of each girder were also applied.

Under the first application of the approximate rated loads for critical loading of the interior girder, the maximum measured bottom-flange stress in the positive-moment region of the interior girder was about equal to the static yield stress. Deformations in the steel girders were barely visible at this load level, and included some additional compression-flange and web distortions in each girder adjacent to the interior pier. This had no effect on the ability of the structure to safely carry the load. The exterior girder $G1$ over the center pier is shown in Figure 10 at the rated AASHTO maximum load. Cracks in the deck system were limited at this load level to the three panels immediately above and adjacent to the interior pier. Crack widths were generally less than 20 mils (0.5 mm). However, separations of the panel joints were observed.

Loading of the bridge continued above the rated AASHTO maximum load. The bridge was able to sustain approximately 240 percent of this rated live load. Although the distortions in the steel girders adjacent to the interior pier gradually increased with the load, the bridge was still able to sustain the increased load. The condition of one exterior girder at 240 percent of the rated AASHTO maximum load is shown in Figure 11. As expected, additional cracking was observed in the precast panels over and adjacent to the interior pier. However, no crushing of the concrete panels was observed at this load.

Loads were also applied for critical loading of the other exterior girder, and similar behavior was observed. The bridge sustained a total live load approximately 220 percent above the rated live load before the test was stopped. Finally, higher-capacity jacks were installed at selected load points and the critical interior-girder loading was reapplied. The bridge then sustained a total live load approximately 250 percent above the rated AASHTO maximum load before concrete crushing was observed in the deck panel at the $^4/_{10}$ point in the west

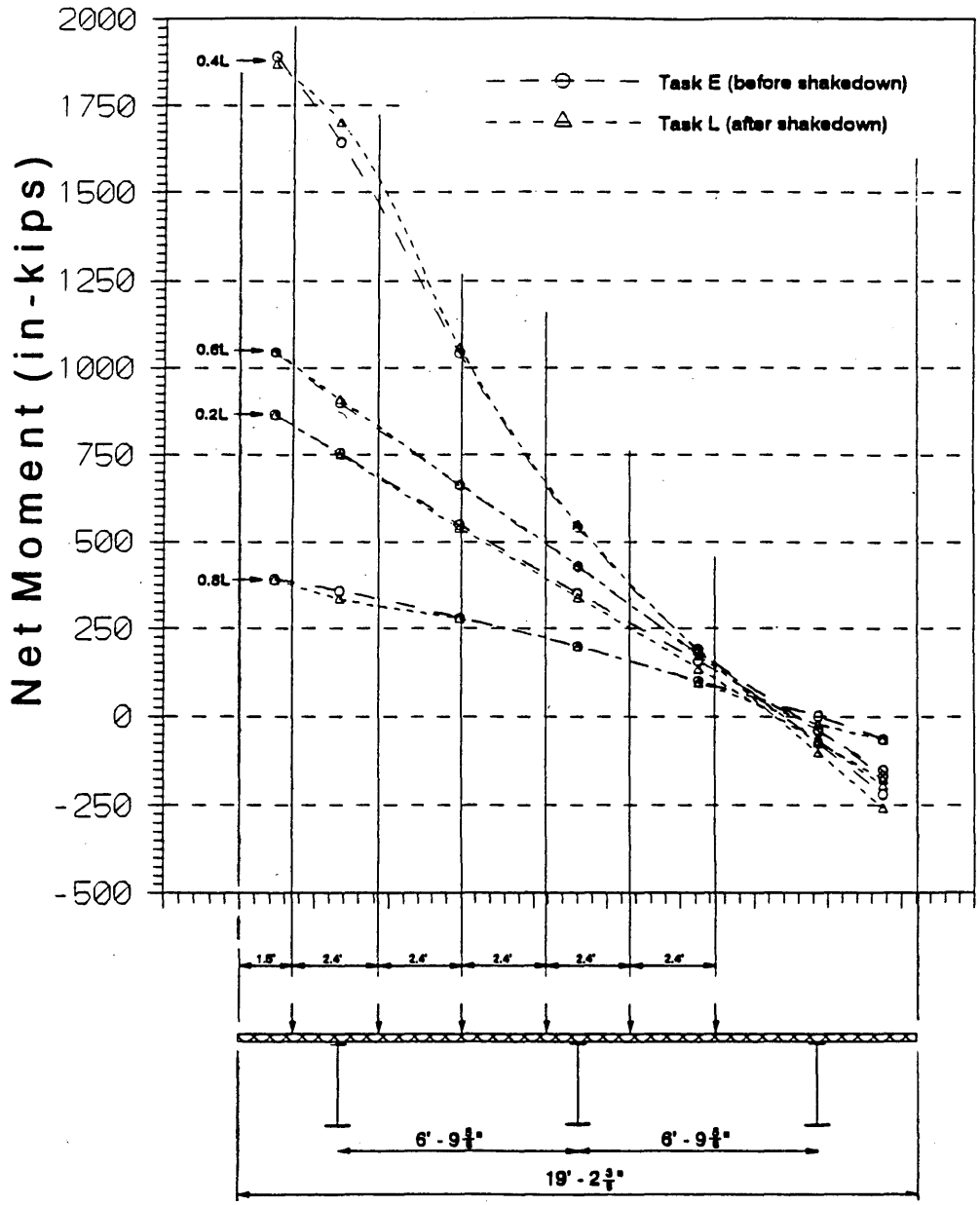

FIGURE 6 Comparison of net moments at 0.4*l* (west span) from measured test data before and after shakedown for exterior girder caused by 16.6 kip concentrated load applied across the bridge at 0.2*l*, 0.4*l*, 0.6*l*, and 0.8*l* (west span).

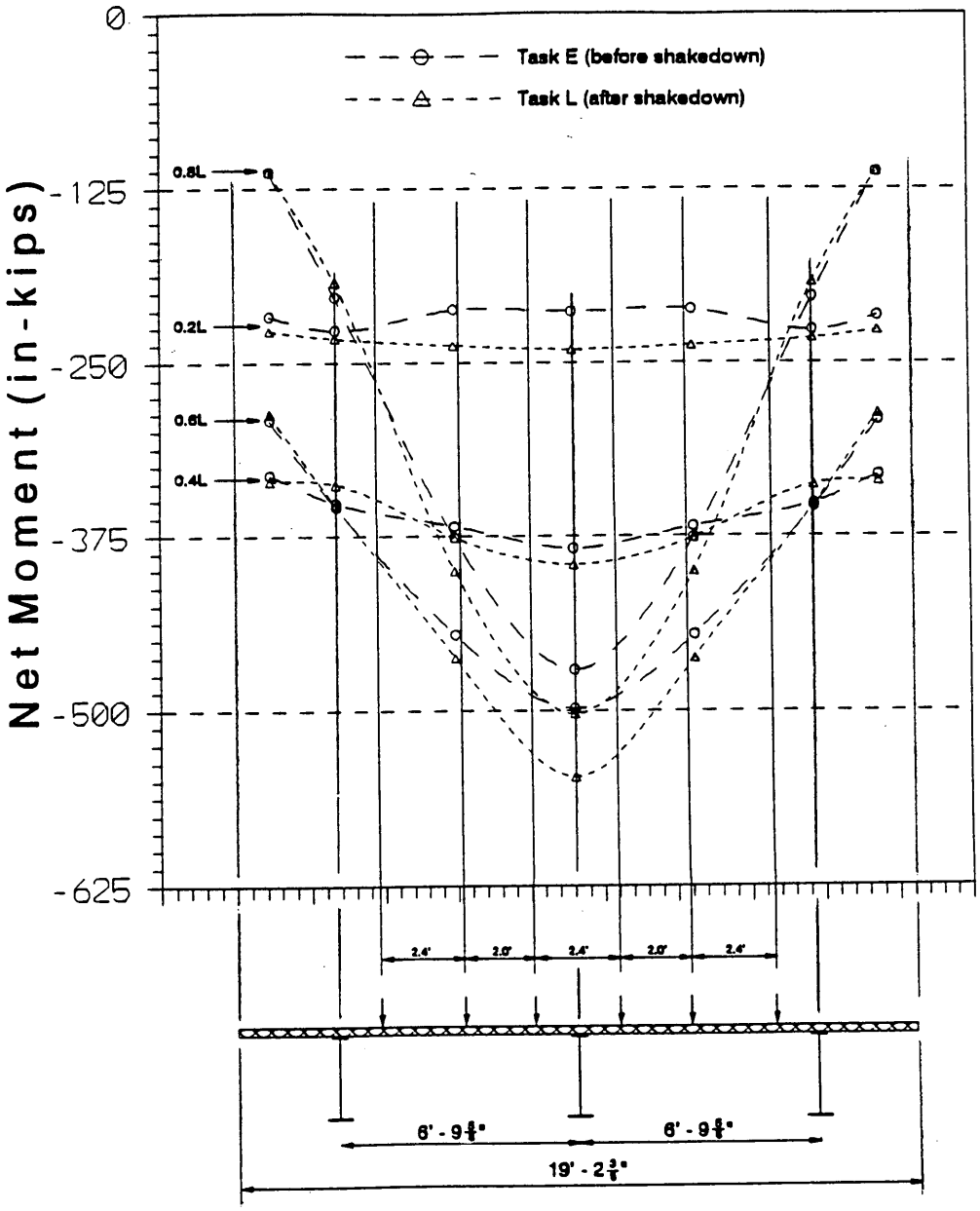

FIGURE 7 Comparison of net moments at 1.0*l* (pier) from measured test data before and after shakedown for interior girder caused by 16.6 kip concentrated load applied across the bridge at 0.2*l*, 0.4*l*, 0.6*l*, and 0.8*l* (west span).

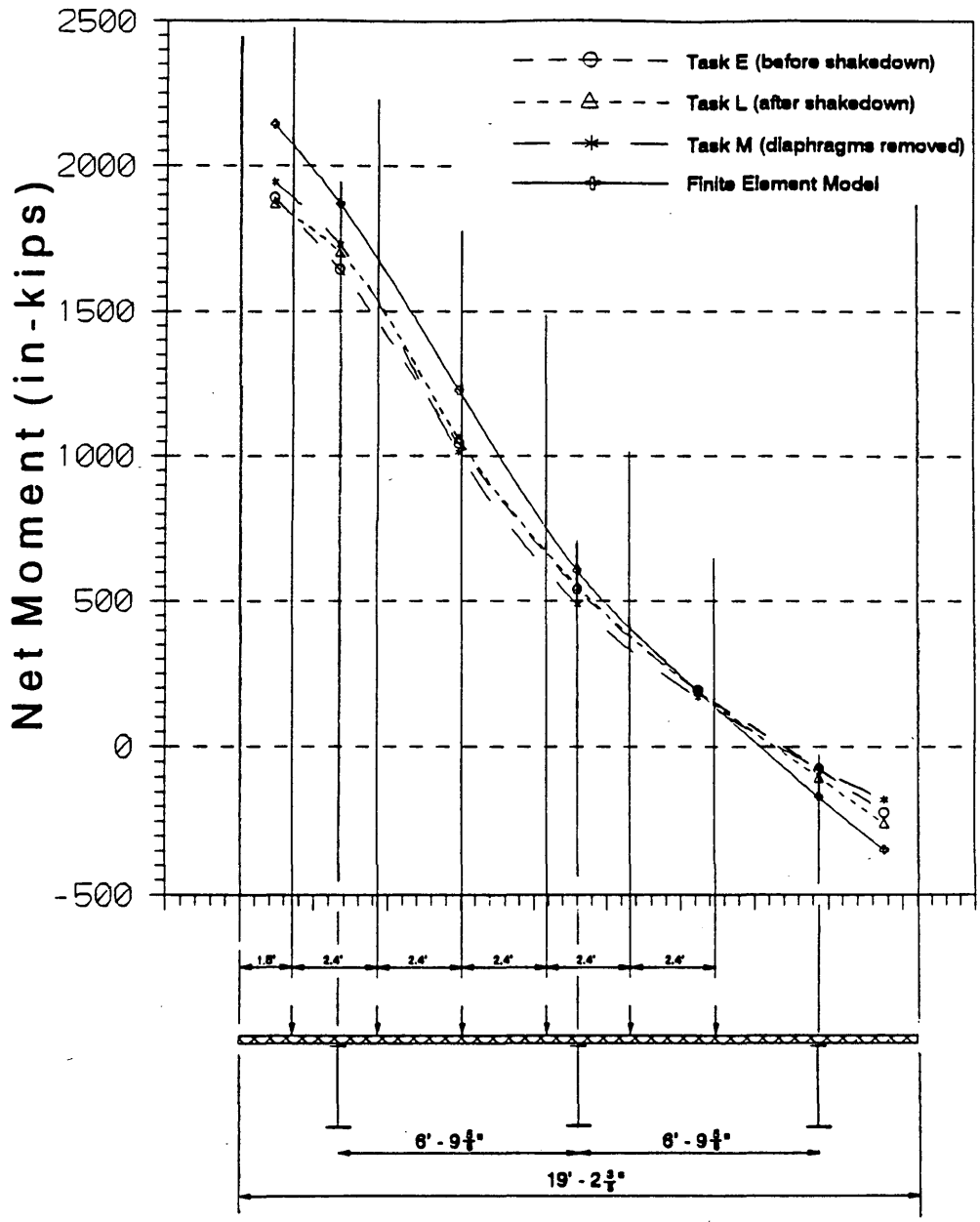

FIGURE 8 Comparison of net moments at 0.4*l* (west span) from measured test data, before and after cross-frames removed, for exterior girder caused by 16.6 kip concentrated load applied across the bridge at 0.4*l* (west span).

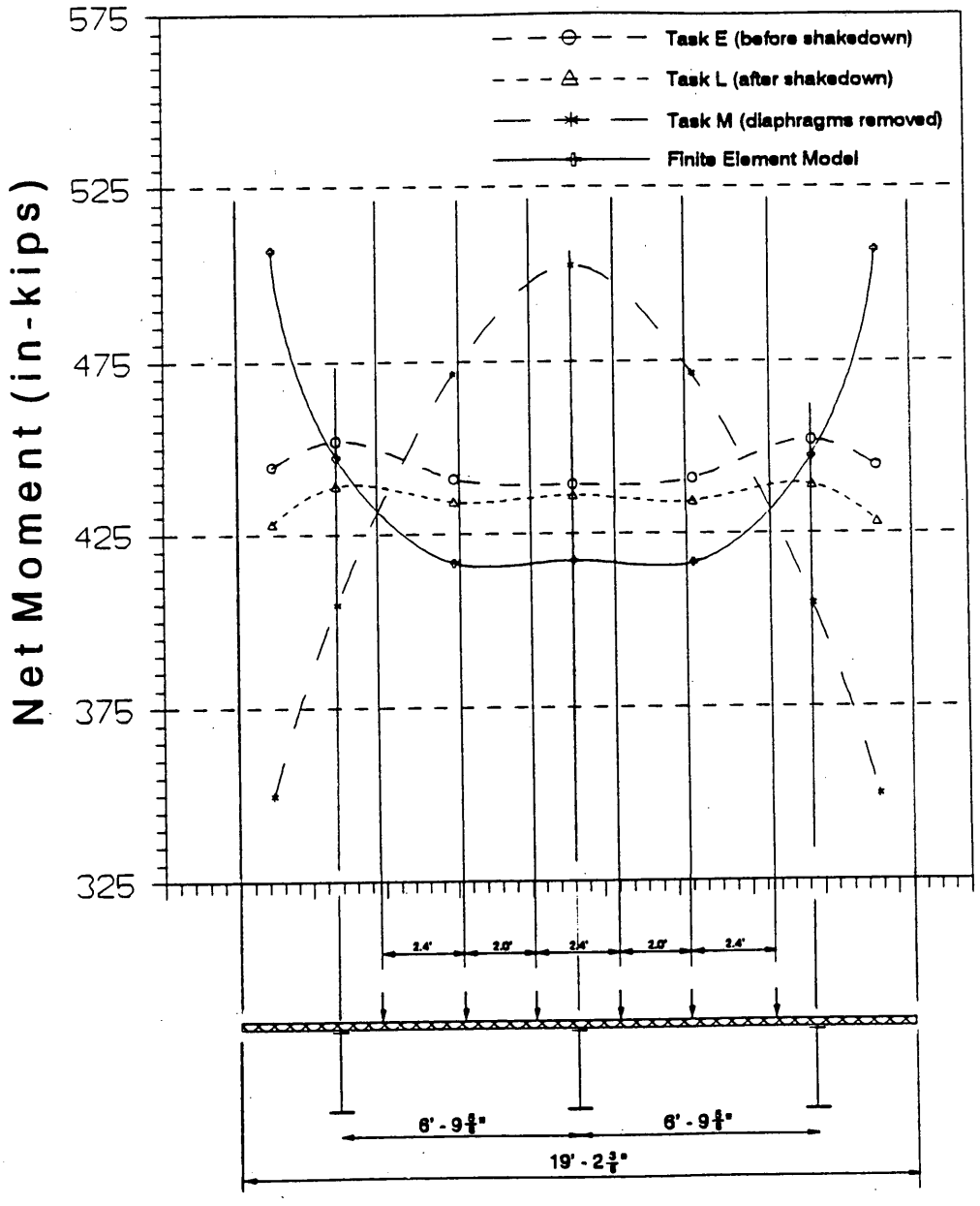

FIGURE 9 Comparison of net moments at 0.6*l* (west span) from measured test data, before and after cross-frames removed, for interior girder caused by 16.6 kip concentrated load applied across the bridge at 0.6*l* (west span).

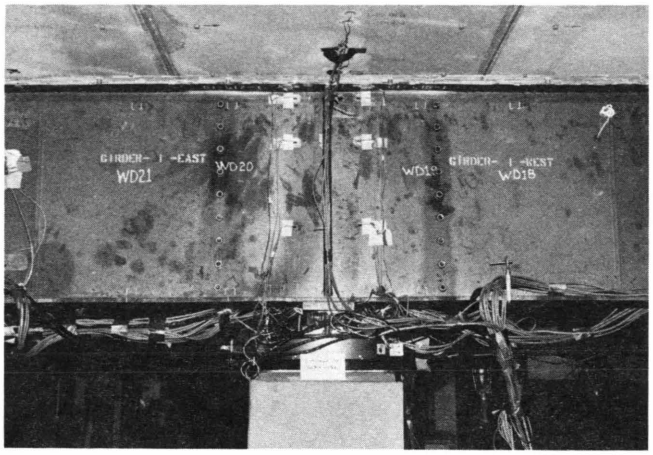

FIGURE 10 Condition of girder *G*1 at pier at 100 percent of rated AASHTO maximum load.

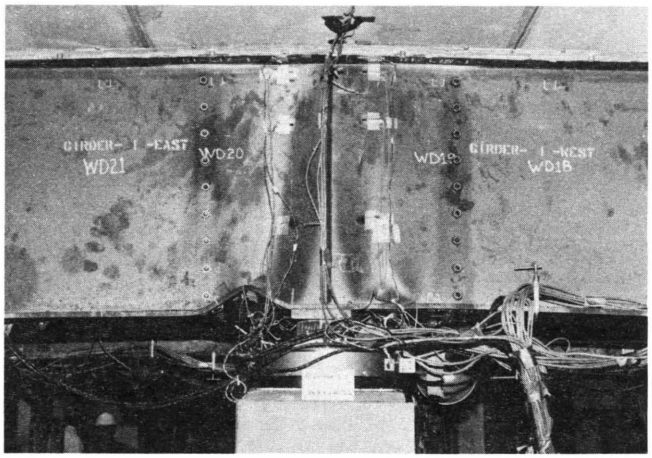

FIGURE 11 Condition of girder *G*1 at pier at 240 percent of rated AASHTO maximum load.

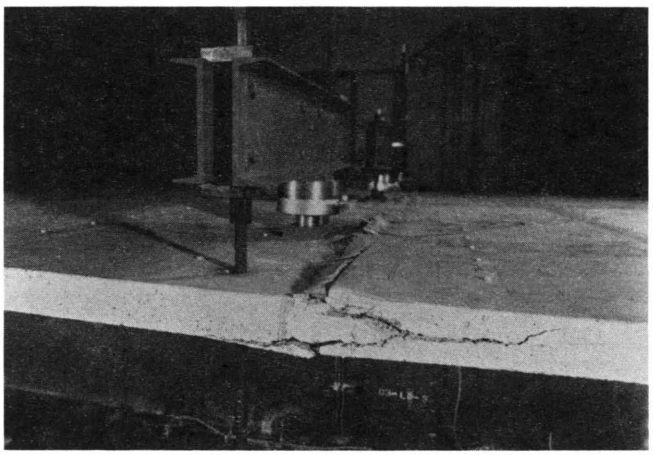

FIGURE 12 Crushing of concrete deck at 0.4*l* of west span.

span as shown in Figure 12. The load-deflection curves from this test to failure are shown in Figure 13.

This series of maximum load tests indicated that significant transverse load sharing occurs among steel girders in a cross section as they are loaded well into the inelastic range. The load sharing is not adequately accounted for by using an elastic lateral wheel-load distribution factor in the maximum load design procedures. The transverse load sharing, along with the available strength in the positive-moment regions and coupled with adequate rotation capacity in the negative-moment regions, resulted in the huge observed reserve strength. Thus, although the ALFD limit-state criteria were more than adequate to meet the maximum load performance requirement for this bridge, the AASHTO equations for maximum load grossly underestimated the strength. An overall view of the model bridge following the maximum load test is shown in Figure 14.

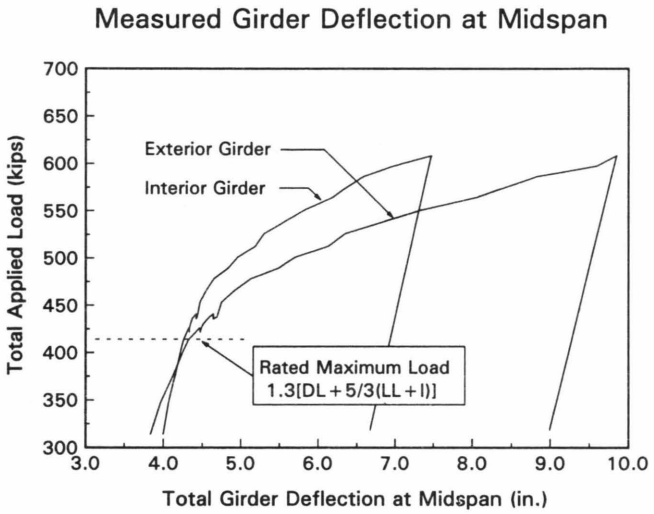

FIGURE 13 Load deflection of girders at maximum load.

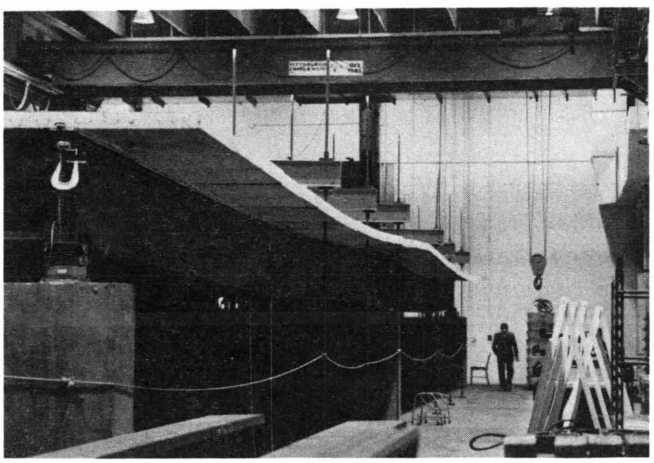

FIGURE 14 Overall view of model bridge loaded to 240 percent of the rated AASHTO maximum load.

CONCLUSIONS

A large experimental test program to evaluate the behavior of a continuous plate-girder bridge, designed according to ALFD (autostress) procedures, with precast prestressed deck panels, has been conducted at the FHWA Turner-Fairbank Highway Research Center in McLean, Virginia. The project was sponsored jointly by AISI and FHWA. A 0.4 scale model of a two-span continuous plate-girder bridge was subjected to a series of tests at each of the three AASHTO load levels: service load, overload, and maximum load. At the service load level, elastic lateral live-load distribution was studied. At the overload and maximum load levels, the adequacy of the ALFD limit-state criteria to satisfy related structural performance requirements was analyzed. The behavior of the concrete slab made of precast deck panels was studied at all three load levels.

At elastic service-load stress levels, live-load lateral-distribution factors for the exterior and interior girders in positive and negative bending were computed from experimentally developed influence surfaces. These factors were compared with factors computed from a finite-element model, from proposed empirical formulas proposed by National Cooperative Highway Research Program Project 12-26, and from present AASHTO procedures. The agreement among the factors computed from the experimental data and a finite element analysis was good. The factors computed from the proposed empirical formulas also gave good agreement with experimental data, especially for the interior girder. However, the proposed formulas did not differentiate between two- and three-lanes loaded. The factors computed using present AASHTO procedures were quite conservative for the interior girder, and less so for the exterior girders. Neither the proposed nor the present AASHTO procedures accounted for the observed variation of the distribution factor along the span. The data indicated that finite-element analysis is a satisfactory method for computing elastic wheel-load distribution factors.

At overload, shakedown with the formation of automoments was observed experimentally. Shakedown was completed in about three cycles of alternating simulated overload truck and lane loading, with the maximum stress in positive bending in the most heavily loaded girder at approximately the limit state of $0.95F_y$. The girders performed satisfactorily with limited local yielding at interior piers. The behavior of precast prestressed modular panels was excellent. Thus, the ALFD limit-state criteria were shown to adequately satisfy the overload structural performance requirement of acceptable riding quality for this bridge.

Elastic influence surface tests and lateral load distribution tests repeated after the overload cycles compared well with identical tests conducted before overload. Elastic behavior was observed in all tests repeated after overload. There was, however, some change in the distribution of loads to the girders, but these changes were less than 7 percent.

At maximum load, the bridge had large reserve strength under simulated maximum load lane loading. It sustained over 2.4 times the ultimate strength determined from AASHTO specifications. The ALFD plastic mechanism analysis method, using effective plastic moment M_{pe}, was adequate to ensure that this bridge had sufficient strength to resist the design loads. The ALFD method did not, however, predict the large reserve strength of the test bridge.

REFERENCES

1. *Guide Specification for Alternate Load Factor Design Procedure for Steel Beam Bridges Using Braced Compact Sections*. American Association of State Highway and Transportation Officials, Washington, D.C., 1987.
2. *Standard Specifications for Highway Bridges*, American Association of State Highway and Transportation Officials, Washington, D.C., 13th Ed., 1989.
3. M. E. Moore, M. A. Grubb, and L. R. Cayes. *Model Bridge Study*. Vol. I, Summary Report. Report FHWA-RD-90-065, FHWA, Washington, D.C., July 1992.
4. M. E. Moore, M. A. Grubb, and L. R. Cayes. *Model Bridge Study*. Vol. II: Component Test Report. Report FHWA-RD-90-066, FHWA, Washington, D.C., Jan. 1991.
5. M. E. Mooore. *Model Bridge Study*. Volume III: Design, Fabrication and Instrumentation. Report FHWA-RD-90-067, FHWA, Washington, D.C., Feb. 1991.
6. M. E. Moore, K. Elnahal, W. S. Hong, P. Albrecht, and M. A. Grubb. *Model Bridge Study*. Volume IV: Service Load, Overload, and Maximum Load Testing. Report FHWA-RD-90-068, FHWA, Washington, D.C., Feb. 1991.
7. M. E. Moore, J. Wang, P. Albrecht, and C. Gilstrap. *Model Bridge Study*. Volume V: Evaluation of Precast Deck Panels. Report FHWA-RD-90-069, FHWA, Washington, D.C., Feb. 1991.
8. M. Moore and I. M. Viest. Laboratory Tests of a Continuous Composite Bridge. In *Proc., Engineering Foundation Conference on Composite Construction*, Henniker, N.H., American Society of Civil Engineers, New York, 1988, pp. 472–486.
9. Highway Research Board *Special Report 61D: The AASHO Road Test, Report 4*, HRB National Research Council, Washington, D.C., 1962.
10. C. G. Schilling. *Moment-Rotation Tests of Steel Bridge Girders*. AISI Project 188, American Iron and Steel Institute, Washington, D.C., April 1985.
11. P. S. Carskaddan, G. Haaijer, and M. A. Grubb. Computing the Effective Plastic Moment. *AISC Engineering Journal*, American Institute of Steel Construction, Chicago, Ill. First Quarter 1982, pp. 12–15.